

A NOVEL METHOD FOR THE DETERMINATION OF $[H_3O^+]$ ION IN STRONG ACIDS VIA CONTINUOUS FLOW INJECTION AND 532NM SOLID STATE LASER DIODE

Issam MA Shakir^{1*} and Ali Q Jameel²

¹Department of Chemistry, College of Science,
University of Baghdad, Baghdad, Iraq,

²Department of research and quality control,
Oil lines pipes Company, Ministry of oil, Baghdad, Iraq.

ABSTRACT

The new method is rapid, simple, and sensitive for the determination of Hydronium ion in strong acids using 532nm solid state laser diode with continuous flow injection analysis and using laser dye (Rhodamine6G) as a fluorescent host. The method was based on the fluorescence of Rhodamine6G and quenching effect of fluorescence by strong acid in aqueous medium. A linear range of strong acid was 7-2000mMol.L⁻¹ for H₂SO₄, 7-1000mMol.L⁻¹ for HNO₃ and 10-2000mMol.L⁻¹ for HCl, with correlation coefficient $r = 0.9750, 0.9791$ and 0.9891 , successively the limit of detection was (LOD) 270.108, 144.608 and 150.616µg/sample based on gradual dilution of lowest concentration in calibration graph. Which are most commonly used strong acids, in various aspects of modern life. Chemical and physical parameters of this system were investigated. The method can be regarded as a unique way of determining acids.

Keywords: Strong acids, Rhodamine6G, Solid state laser.

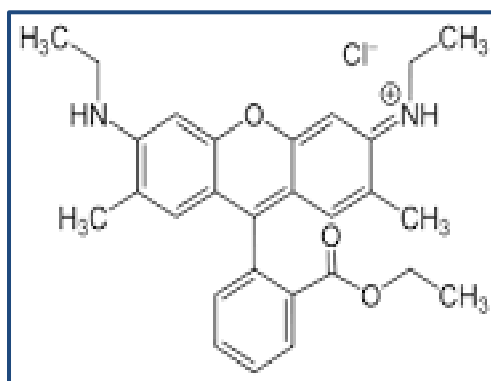


Fig. 1: Rhodamine6G Structure

1. INTRODUCTION

A strong acid is a good proton (H^+) donor that completely dissociates in water; in other words, one mole of a strong acid HB dissolves in water yielding one mole of H^+ and one mole of the conjugate base B^- and none of the protonated acid HB . Examples of strong acids are hydrochloric acid, perchloric acid, nitric acid and sulfuric acid¹. Some of the most commonly used methods for

determination of strong acids include potentiometric titration², spectrophotometry³, gas⁴ chromatographic and flow injection analysis⁵⁻⁹.

Rhodamine6G is used as a laser dye, or gain medium, in dye lasers,^{10,11} and is pumped by the 2nd (532 nm) harmonic from an Nd:YAG laser. The dye has a remarkably high photostability, high fluorescence quantum yield, low cost, and its lasing range has close proximity to its absorption maximum (approximately 530 nm)^{12,13}. The emission range of the dye is 555 to 585 nm with a maximum at 566 nm. Rhodamine6G usually comes in three different forms¹⁴. Rhodamine6G chloride is a bronze/red powder, highly soluble¹⁵, this formulation is very corrosive to all metals except stainless steel. Other formulations are less soluble, but also less corrosive. Rhodamine6G perchlorate comes in the form of red crystals, while Rhodamine6G tetrafluoroborate appears as maroon crystals^{16,17}. Solid-state lasers are lasers based on solid-state gain media such as crystals or glasses doped with rare earth or transition metal ions, or semiconductor lasers. (Although semiconductor lasers are of course also solid-state devices, they are often not included in the term solid-state lasers.) Ion-doped solid-state lasers (also sometimes called doped insulator lasers) can be made in the form of bulk lasers, fiber lasers, or other types of waveguide lasers. Solid-state lasers may generate output powers between a few milliwatts and (in high-power versions) many kilowatts^{18,19}. Many solid-state lasers are optically pumped with flash lamps or arc lamps. Such pump sources are relatively cheap and can provide very high powers. However, they lead to a fairly low power efficiency, moderate lifetime, and strong thermal effects such as thermal lensing in the gain medium. For such reasons, laser diodes are very often used for pumping solid-state lasers. Such diode-pumped solid-state lasers (DPSS lasers, also called all-solid-state lasers) have many advantages, in particular a compact setup, long lifetime, and often very good beam quality. Therefore, their share of the market is rapidly rising^{20,21}.

2. Experimental

2.1. REAGENTS AND CHEMICALS

A stock solution (0.01 Mol.L⁻¹) of Rhodamine6G (C₂₈H₃₁N₂O₃Cl, M.Wt 479.02 g.mol⁻¹) was prepared by dissolving 2.3951g in 500 ml of distilled water. A stock solutions of acids Sulphuric acid (98%w/w, 1.84 g.ml⁻¹, BDH, 2Mol.L⁻¹), Nitric acid (70% w/w, 1.42g.ml⁻¹ BDH, 2Mol.L⁻¹) and Hydrochloric acid (38%, 1.18g.ml⁻¹, Fluka, 2Mol.L⁻¹) was prepared by pipetting 108.78ml, 126.78ml, 162.63ml and respectively of concentrated acids and complete the volume with distilled water to 1000 ml volumetric flasks. Hydrochloric acid was standardized against standard solution from Na₂CO₃ (BDH, 105.9g.mol⁻¹ 0.1Mol.L⁻¹); which prepared by dissolving 2.6498g in 250 ml distilled water and (Sulphuric acid, Nitric acid) was standardized against standard solution from NaOH (BDH, 40 g.mol⁻¹ 0.1Mol.L⁻¹); which prepared by dissolving 1g in 250 ml distilled water.

2.2. Apparatus

Laser diode fluorimeter is a homemade instrument that is capable in measuring fluorescence at 405(10mW), and 532nm(not less than 1000mW) laser diode. Both radiation source is fitted with a 2mm flow cell in a block of brass metal equipped with a photo diode detector. The angle between the radiation source at an aperture of 2mm a maximum radiation area for a flow cell having outside diameter 4mm inside diameter 2mm (path length for absorption of irradiation) is 90°. The whole instrument composed of five main parts which are as follows: Fluorescence cell, Flow cell, detector, irradiation sources and general panel of instrument. It is possible that the operation of each single light source can be done separately (i.e.; individual mode) or there is a possibility of working both (this gives the analyst a wide choice using two wave length for the same solution. Also in the front panel there are two outlets for the signals to receive the output from each individual unit (i.e.; either 405nm unit or 532nm laser or both). When the turn unit, are joints intensity (i.e.; the sample leaving the 405nm unit will pass to 532nm unit then leaves the instrument. All tubes are made of Teflon 1mm inside diameter 2mm outside. One channel of peristaltic pump was used (Ismatec type ISM 796), A rotary 6-port injection valve (Rheodyne, U.S.A) with a sample loop (id 1 mm, Teflon, Variable length) used for sample injection. The output signals was recorded by x-t potentiometric recorder (KOMPENSO GRAPH C-1032) Siemens (Germany).

2.3. Methodology

The general procedure will be the use of 532nm solid state diode laser (green laser) as it will be discussed for creation of various different studies that will be adopted (e.g.; variable studies) scatter plot was first to made followed by selecting the calibration curve most acceptable level of correlation coefficient decided by the researcher and the outcome of the obtained data from the measurements. Every signal measurement was repeated for three successive times. Repeatability and limit of

detection were carried out. Three different acids were studied Sulphuric, Nitric, and Hydrochloric as strong inorganic acid. As these acids describes the most commonly used inorganic acid. The flow diagram of the whole reaction manifold system used for the determination of Hydronium ion in strong acids by the reaction between strong acids and Rhodamine6G to fluorescence quenching. The carrier stream (Rhodamine6G) ($1.1 \times 10^{-4} \text{ Mol.L}^{-1}$) at 2 mL.min^{-1} flow rate to react with the injected sample volume ($459 \mu\text{l}$) strong acids and carry the mixture to complete the reaction. This segment passes through flow measuring cell. The response profile of which was recorded on x-t potentiometric recorder to measure quenching of fluorescence expressed as peak height in mV.

3. Optimization of experimental conditions

A series of experiments were conducted to establish the optimum parameters. Chemical variables such as reagents concentration, as well as physical variables including flow rate, purge time, recharging build up time and injected sample volume were investigated.

3.1 Chemical variables

3.1.1. Choice of Rhodamine6G concentration for most favorable fluorescence intensity using 532 nm solid state laser.

It was quite necessary to decide between two modes of operation to describe this project. Two choices were to choose from. Sensitivity, ease of operation (manipulation), consumption of reagent (chemical used, in this case Rhodamine6G), time of measurement, repeatability and simplicity of the manifold design.

The first mode of operation based on creation of fluorescence on a constant level of obtained fluorescence intensity i.e.; continuous mode of operation i.e.; quenching of fluorescence i.e.; process that can lead to a reduction in fluorescence intensity on the flow gram is shown in figure no.(2). While in Figure no.(3): shows the discrete mode of operation i.e.; inhibition of fluorescence i.e.; slowing the activity or occurrence of fluorescence.

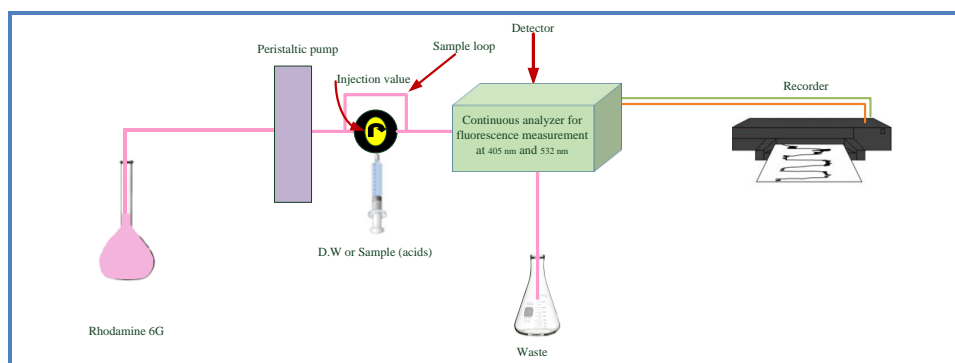


Fig. 2: Flow gram of manifold based on Continuous mode i.e.; quenching of fluorescence

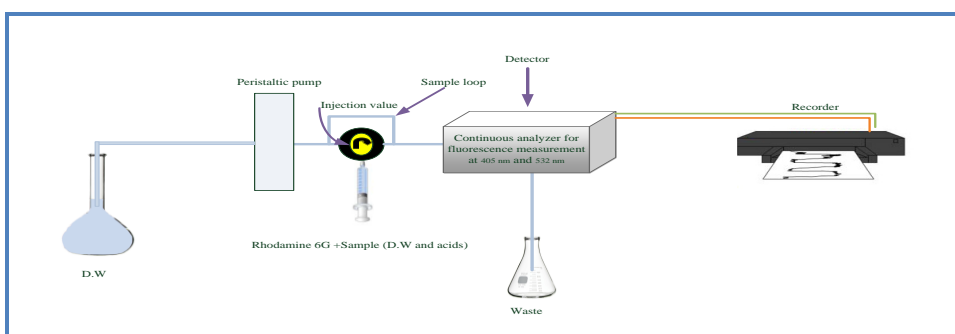


Fig. 3: Flow gram of manifold based on Discrete mode i.e.; inhibition of fluorescence

3.1.1.1. Continuous mode of operation (quenching of fluorescence)

In order to evaluate the methodology that is to be adopted through the research work. Rhodamine6G have the tendency of being adsorbed by the many kind of tube material or either standing the prepared solution for a while or not freshly prepared.

Variable concentration (1×10^{-6} $5 \times 10^{-4} \text{ Mol.L}^{-1}$) of Rhodamine6G was prepared from a stock solution of $1 \times 10^{-2} \text{ Mol.L}^{-1}$ (2.3951g/500ml) indistilled water. Figure no.(4) shows the profile of fluorescence intensity vstime of three Variable concentration of Rhodamine6G. While table no(1). Tabulates all the data obtained i.e.; peak height mV, standard deviation, and confidence interval of average peak heights. Figure no (5) shows the fluorescence intensity expressed by peak height mV for three successive measurements of the used Rhodamine6G concentration. It indicate that there is an approximate linear increase of the fluorescence intensity for 1×10^{-6} - $5 \times 10^{-5} \text{ Mol.L}^{-1}$ gave a robust equation of the form $a + b x = 414.15 + 26415094 x$ while correlation coefficient having the value of 0.7911. The slope indicate a quick sensitive rise of the intensity. While the part of the curve in Figure no.(5) that expressed from 1×10^{-4} -- $5 \times 10^{-4} \text{ Mol.L}^{-1}$ indicate a value of correlation coefficient of 0.2361, and value of $a = 1717.6528$ and slope of 25427.87 which is less sensitive by a factor of 9.626×10^{-4} ($\approx 10000X$) than the part A in the same figure. Therefor part B is regarded as the best optimum peak height that can be used throughout this work. Any concentration in the part B could be used. It is not quite necessary that the researcher should stick to the prepared measured points.

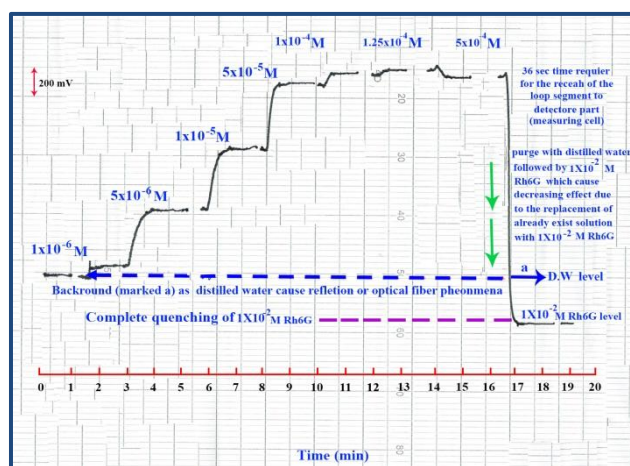


Fig. 4: Fluorescence intensity expressed as mV transducer output vs time. Using continuous mode of operation (i.e.; Quenching of released fluorescence)

Table 1: fluorescence intensity expressed as mV of average peak height,(n=3) of variable Rhodamine6G concentration

Concentration of Rhodamine6G in distilled water (Mol.L^{-1})	Average (\bar{y}_i) (mV)	Standard deviation (S.D) σ_{n-1}	RSD %	Confidence interval of the mean at 95% $\bar{Y} \pm t \text{ sem}$
1×10^{-6}	100	0	0	100 ± 0
5×10^{-6}	560	1	0.18	560 ± 2.49
1×10^{-5}	1080	3	0.28	1080 ± 7.46
5×10^{-5}	1660	10	0.60	1660 ± 24.87
1×10^{-4}	1740	10	0.57	1740 ± 24.87
1.25×10^{-4}	1760	0	0	1760 ± 0
5×10^{-4}	1700	0	0	1700 ± 0

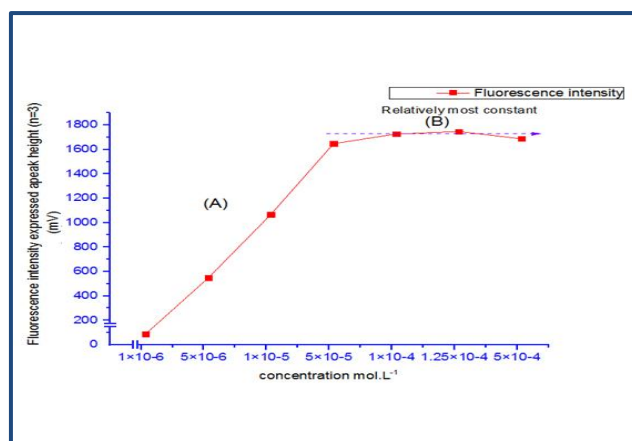


Fig. 5: Variation of fluorescence intensity expressed as mV transducer response v.s concentration of Rhodamine6G Using continuous mode of operation i.e.; (Quenched fluorescence)

3.1.1.2. discrete mode of operation (inhibition of fluorescence).

Proceeding as in section A. Variable response were obtained as shown in Figure no.(6) while table no.(2) tabulate the results obtained. It can be noticed that through plotting the output of irradiation process gave two segment arising segment as shown in figure no.(7). A step increase in sensitivity followed by 2nd segment nearly as plateau a choice at this stage will be on part B in the same figure.

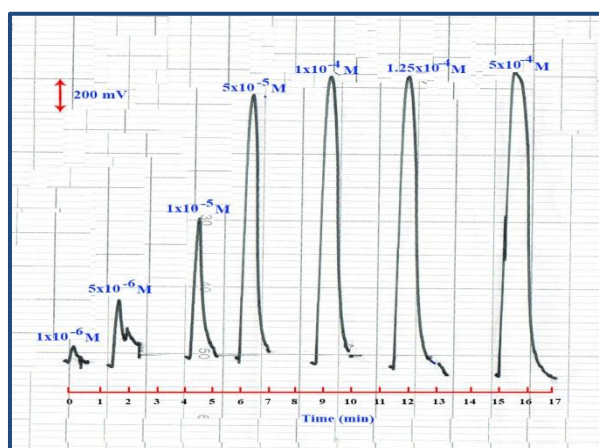


Fig. 6: Fluorescence intensity expressed as mV transducer output vs time. Using discrete mode of operation (i.e.; inhibition of released fluorescence)

Table 2: Fluorescence intensity expressed as mV of average peak height, (n=3) of variable Rhodamine6G concentration

Concentration of Rhodamine6G in distilled water (Mol.L ⁻¹)	Average (\bar{y}_i) (mV)	Standard deviation (S.D.) σ_{n-1}	RSD %	Confidence interval of the mean at 95% $\bar{Y} \pm t \text{ SEM}$
1×10^{-6}	120	0	0	120 ± 0
5×10^{-6}	500	0	0	500 ± 0
1×10^{-5}	1060	20	1.89	1060 ± 49.75
5×10^{-5}	1960	10	0.51	1960 ± 24.87
1×10^{-4}	2180	5	0.23	2180 ± 12.44
1.25×10^{-4}	2180	10	0.46	2180 ± 24.87
5×10^{-4}	2300	0	0	2300 ± 0

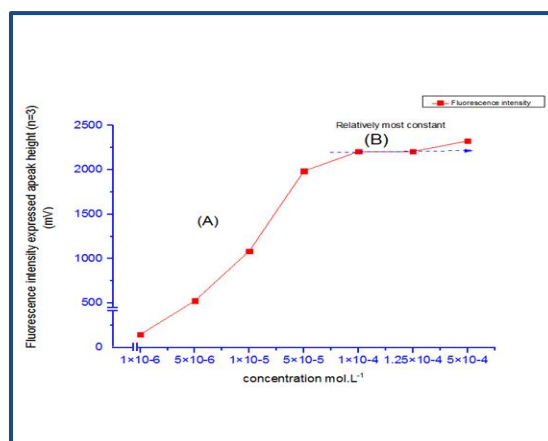


Fig. 7: Variation of fluorescence intensity expressed as mV transducer response. vs concentration of Rhodamine6G. Using discrete mode of operation – i.e.; (inhibition of fluorescence)

3.1.1.3. Mode of operation to choose from

From the above all mentioned experimented parameter the moment of decision has come to choose either a quenched fluorescence process i.e.; continuous mode or an inhibition process i.e.; discrete mode. A continuous mode was the choice.

The whole research work will be based on a constant feed of Rhodamine6G as a carrier stream while injecting sample solutions that supply necessary feed of fluorescence molecule via six port injection valve on a carrier stream as shown in figure (2)

The working profile for the adopted methodology is to record signal of distilled water followed by change of the carrier stream to Rhodamine6G solution; a sudden rise will be produced due to irradiation by solid state laser at 532 nm and a release of fluorescence of yellow – orange colour (555nm). Since total fluorescence will be captured by the used detector. A constant and stable signal signs the start of using samples to be injected and to record the energy transducer output signal. All obtained signal is subtracted from distilled water signals are measurement for three successive time as a general issue.

3.1.2. Effect of stability of Rhodamine6G with standing time

An experiment was conducted using 1.1×10^{-4} Mol.L⁻¹ of Rhodamine6G solution to describe whether Rhodamine6G solution losses some of its concentration via either decomposition while in water or loss some of its strength due to adsorption on the glass containers (i.e.; volumetric flask). Table no.(3) tabulated the fluorescence intensity of Rhodamine6G solution after \approx zero time (intensity prepared or freshly prepared solution), 24 hours, 48 hours, and 72 hours. Then was a decrease of fluorescence intensity with time which did not exceed 12.14% for a solution prepared before three days. Figure no.(8) shows kind of response on a continuous mode base (i.e.; quenched fluorescence). On the above mentioned, experiment and its result one might conclude to use all we go freshly prepared solution. That will be mode of working methodology unless otherwise stated.

Table 3: Effect of standing time of prepared solution of Rhodamine6G vs fluorescence intensity

Time (hr)	average (mV)	σ_{n-1}	RSD%	$\bar{Y} \pm t \text{ sem}$	Error %
0	2800	20	0.71	2800 ± 49.75	0%
24	2593	11.55	0.45	2593 ± 28.73	-7.38%
48	2520	20	0.79	2520 ± 49.75	-10%
72	2460	20	0.81	2460 ± 49.75	-12.14%

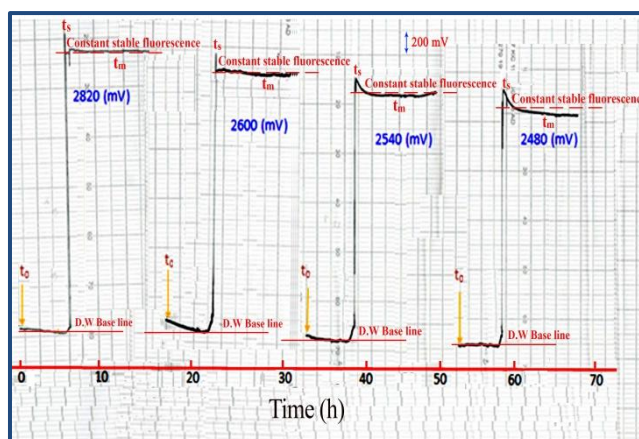


Fig. 8: profile of Fluorescence intensity vs time using continuous mode (quenched mode) Of Rhodamine6G ($1.1 \times 10^{-4} \text{ Mol.L}^{-1}$)

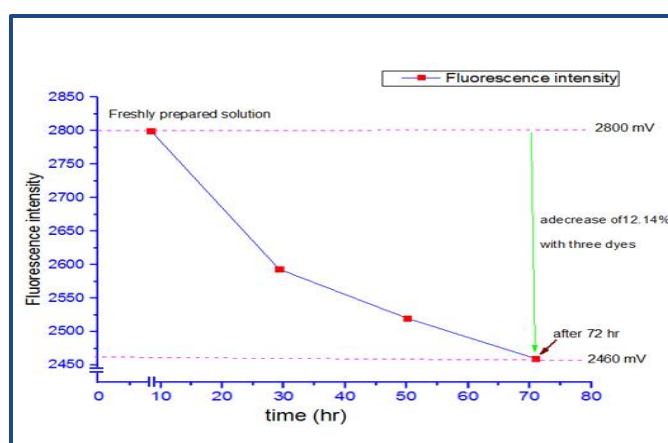


Fig. 9: Variation of fluorescence intensity of Rhodamine6G ($1.1 \times 10^{-4} \text{ Mol.L}^{-1}$) with time (days)

3.2. Physical variables

3.2.1. Flow rate

Different flow rate were tried starting with lowest flow rate which is equivalent to 1 ml.min^{-1} . Figure no.(10) shows various response of quenched fluorescence response recorded on a continuous mode of operation. Table no.(4) describes the average energy transducer response, standard deviation, and confidence intervals of all data obtained. Figure no.(11) plot of average three successive response vs flow rate clearly indicate that 2 ml.min^{-1} gave relatively higher response that this research work will rely on it and will be used throughout all applications.

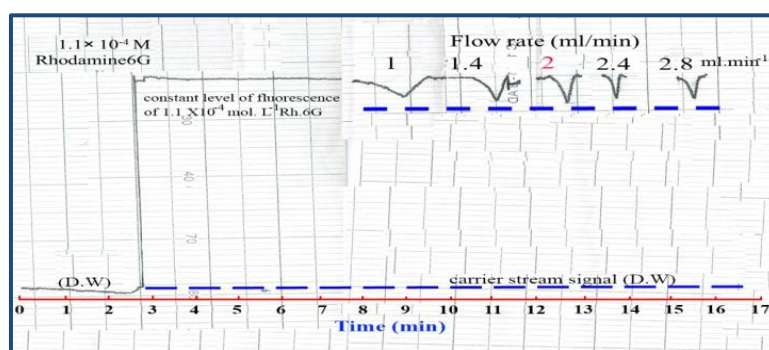
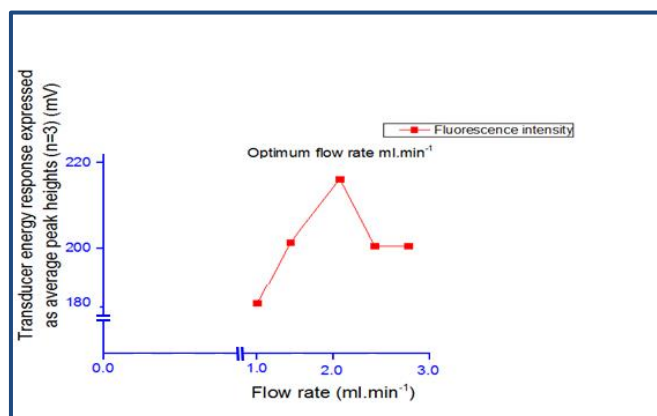


Fig. 10: Profile of continuous mode of quenched fluorescence showing a constant level of fluorescence and the quenched effect caused by distilled water at variable flow rates.

Table 4: Variation of flow rate and it effect on fluorescence intensity

Flow Rate ml.min ⁻¹	Y _i (mV)	S.D σ_{n-1}	RSD %	$\bar{Y} \pm t \text{ sem}$	Δt_b^{**} (sec)	t^{***} (sec)
1	180	0	0	180 \pm 0	120	30
1.4	200	0	0	200 \pm 0	60	24
2	220	2	0.909	220 \pm 4.975	36	12
2.4	200	1	0.5	200 \pm 2.487	36	12
2.8	200	3	1.5	200 \pm 7.462	30	6

**Fig. 11: A plot variation of constant continuous mode of fluorescence response verses flow rate (ml.min⁻¹)**

3.2.2. Effect of variation of sample volume on the fluorescence created by continuous mode of operation

Using the optimum flow rate of 2 mL.min⁻¹ with constant loop internal diameter (1mm) via the use of different sample volumes. Figure no (12) shows the exact energy transducer response of the fluorescence of Rhodamine6G (1.1×10⁻⁴ Mol.L⁻¹) with distilled water. Table no.(5) tabulated all data concerned with measurement.

Table 5: Effect of variation of sample volume on quenching of Fluorescence intensity of Rhodamine6G (1.1×10⁻⁴) Mol.L⁻¹

Sample volume* (ml) via choice of variable loop lengths	Y _i (mV)	S.D σ_{n-1}	RSD %	$\bar{Y} \pm t \text{ sem}$	Δt_b^{**} (sec)	t^{***} (sec)
0.020	0	0	0	0 \pm 0	0	0
0.137	60	1	1.667	60 \pm 2.487	12	6
0.216	80	1	1.25	80 \pm 2.487	18	12
0.294	100	2	2	19.833 \pm 4.975	24	18
0.381	140	0	0	140 \pm 0	24	18
0.459	200	1	0.5	200 \pm 2.487	30	36

*The volume indicate is calculated (3decimal approximation) from tube length of and tube diameter as used in this research work via volume of cylinder $[\pi \cdot (\text{diameter}/2)^2 \cdot \text{tube length}(L)]$.

**Peak base width.

***Time for the detector to detect the starting of the signal. ($t_0 - t_s$) where t_0 material injection while t_s = Start of the response.

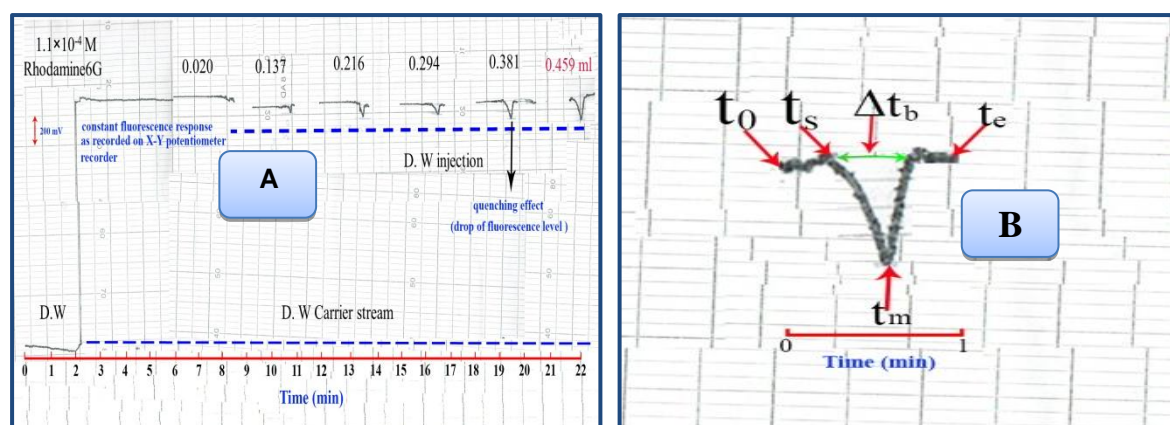


Fig. 12 A,B: effect of sample volume on fluorescence intensity response v.s with time

t_0 : Time in used of second start injected the sample.(turn on the valve)

t_s : Starting of the signal time required to reach.

t_m : Maximum response of the signal.

t_e : Total time where response ends (diminish).

3.2.4.Purge time of the Injected Sample.

Purge time can be defined as the total time required to discharge of all sample that is the variable in the sample loop. This definition should take into account flow rate and sample volume (loop length and diameter length). Table no.(6) tabulated all obtained data for continuous mode of fluorescence (quenched fluorescence). The level indicate clearly that open valve mode will contribute to the stability of the obtained signal fluorescence. Therefor on the basis open valve mode will be adopted throughout the research work.

Table 6:Effect for the variation of purge time on the quenching of Fluorescence intensity of Rhodamine6G (1.1×10^{-4}) Mol.L⁻¹

Purge time (sec)	\bar{Y}_i (mV)	S.D σ_{n-1}	%RSD	$\bar{Y} \pm t \text{ sem}$	Δt_b^{**} (sec)	t^{***} (sec)
10	140	2	1.43	140 ± 4.97	18	12
20	200	0	0	200 ± 0	30	18
30	200	0	0	200 ± 0	30	18
40	200	1	0.5	200 ± 2.49	36	12
Open valve > 40	220	1	0.46	220 ± 2.49	30	12

4.Calibration graph of strong acids

4.1.Calibration graph of Sulfuric acid (H₂SO₄)

A series of sulfuric acid solutions ranging from (7 to 2000) mMol.L⁻¹ were prepared from a stock solution having the concentration of 2Mol.L⁻¹ in distilled water and injected at the established optimum conditions(c.f.section3) All range used can be regarded as no significant different i.e.; since r values are regarded as more than good which indicate that the used equation $Y = a + bx$ was able to explain 95.07% for $r = 0.9750$ to 97.91% for $r = 0.9895$

A compromise between used concentration range and resultant r values should be taken into account when using any of the above concentration range.A sample of fluorescence intensity vs time profile can be seen in figure no.(16).

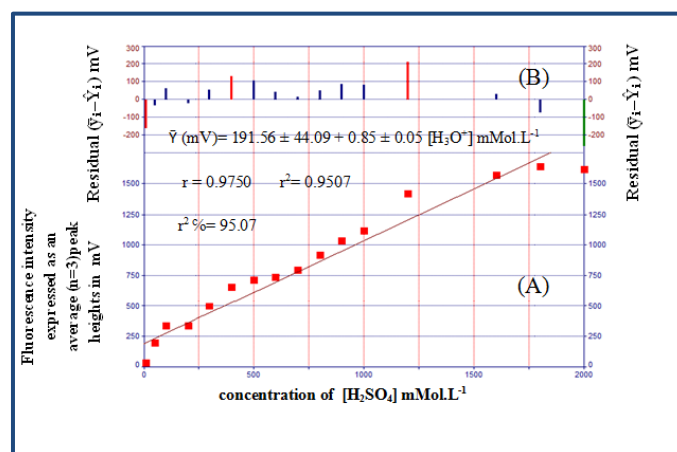
Table 7: Scatter data (i.e.; all measured data for Sulphuric acid)

Concentration of H ₂ SO ₄ in distilled water (mMol.L ⁻¹)	\bar{Y}_i mV	S.D σ_{n-1}	RSD %	$\bar{Y} \pm t \text{ sem}$
7	35	0	0	35 \pm 0
9	40	0	0	40 \pm 0
10	40	0	0	40 \pm 0
50	200	0	0	200 \pm 0
100	340	0	0	340 \pm 0
200	338	2.89	0.86	338 \pm 7.19
300	500	0	0	500 \pm 0
400	660	0.58	0.09	660 \pm 1.44
500	720	0	0	720 \pm 0
600	740	0	0	740 \pm 0
700	798	2.89	0.36	798 \pm 7.19
800	920	0	0	920 \pm 0
900	1040	0.57	0.05	1040 \pm 1.44
1000	1120	0	0	1120 \pm 0
1200	1420	0	0	1420 \pm 0
1600	1575	5	0.32	1575 \pm 12.44
1800	1640	0	0	1640 \pm 0
2000	1620	0	0	1620 \pm 0

Variation range was used in order to choose the most acceptable level that will describe the work conducted using 532nm solid state diode laser (green laser). Table no. (8) shows these values.

Table 8: Linear range and it is associated correlation coefficient for Sulfuric acid

Range of used concentration mMol.L ⁻¹	Correlation coefficient (r)	r ² %	Shown in
7-2000	0.9750	95.07	Fig no. 4.1
7-1800	0.9823	96.49	Fig no 4.2
10-1800	0.9840	96.82	Fig no 4.3
50-1600	0.9895	97.91	Fig no 4.4

**Fig. 13: Scatter plot for the variation of H₂SO₄ concentration on: A- Fluorescence intensity, B- residual ($\bar{Y}_i - \bar{Y}_i$)**

4.2. Calibration graph of Nitric acid (HNO₃)

A series of Nitric acid solutions ranging from (7 to 2000) mMol.L⁻¹ were prepared from a stock solution having the concentration of 2Mol.L⁻¹ in distilled water and injected at the established optimum conditions (c.f. section 3). The first range used (7-2000) which gave a correlation coefficient $r = 0.8041$ with an explained values for all data given to be 64.65%. This is regarded a weak correlation for equation used $Y = a + bx$. While the second and third range used can be regarded as no significant different i.e.; since r values are regarded as more than good which indicate that the used equation $Y = a + bx$ was able to explain 95.87% for $r = 0.9791$ to 96.76% for $r = 0.9837$.

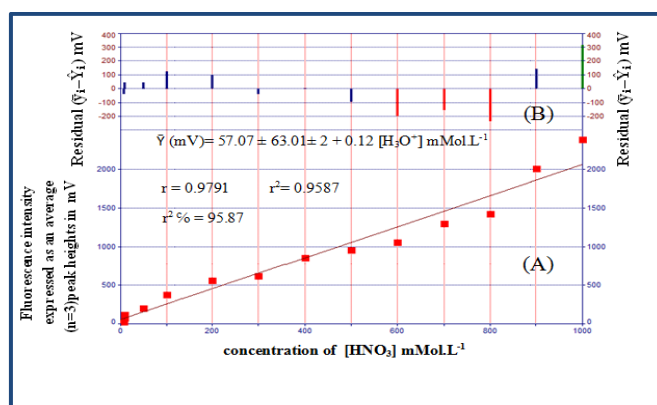
A compromise between the second and third used concentration range and resultant r values should be taken into account when using any of the above concentration range. A sample of fluorescence intensity vs time profile can be seen in figure no. (16).

Table 9: Scatter plot data (i.e.; all measured data were used for linear regression)

Concentration of HNO ₃ in distilled water (mMol.L ⁻¹)	\bar{Y}_i mV	S.D σ_{n-1}	RSD %	$\bar{Y} \pm t \text{ sem}$
7	30	0	0	30 \pm 0
9	80	0	0	80 \pm 0
10	120	0	0	120 \pm 0
50	200	0	0	200 \pm 0
100	380	0	0	380 \pm 0
200	557	2.89	0.52	557 \pm 7.19
300	617	2.89	0.47	617 \pm 7.19
400	860	0	0	860 \pm 0
500	960	0	0	960 \pm 0
600	1060	0	0	1060 \pm 0
700	1303	2.89	0.22	1303 \pm 7.19
800	1423	2.89	0.20	1423 \pm 7.19
900	2003	5.77	0.29	2003 \pm 14.35
1000	2377	5.77	0.24	2377 \pm 14.35
1200	1140	1	0.09	1140 \pm 2.49
1500	1375	5	0.36	1375 \pm 12.44
1800	1680	0	0	1680 \pm 0
2000	1775	5	0.28	1775 \pm 12.44

Table 10: Range of the used concentration for Nitric acid

Range of used concentration (mMol.L ⁻¹)	Correlation coefficient (r)	r ² %
7-2000	0.8041	64.65
7-1000	0.9791	95.87
7-900	0.9837	96.76

**Fig. 14: Calibration graph obtained from Scatter plot for the variation of HNO₃ concentration on:
A- Fluorescence intensity, B- residual ($\bar{y}_i - \hat{Y}_i$).**

4.3. Calibration graph of Hydrochloric acid (HCl)

A series of Hydrochloric acid solutions ranging from (10 to 2000) mMol.L⁻¹ were prepared from a stock solution having the concentration of 2Mol.L⁻¹ in distilled water and injected at the established optimum conditions. Two range used can be regarded as no significant different i.e.; since r values are regarded as more than good which indicate that the used equation $Y = a + bx$ was able to explain 97.83% for $r = 0.9891$ to 98.23% for $r = 0.9911$.

A compromise between used concentration range and resultant r values should be taken into account when using any of the above concentration range. A sample of fluorescence intensity vs time profile can be seen in figure no.(16).

Table 11: Scatter plot data (i.e.; all measured data were used for linear regression).

Concentration of HCl in distilled water (mMol.L ⁻¹)	\bar{Y}_i mV	S.D σ_{n-1}	RSD %	$\bar{Y} \pm t \text{ sem}$
10	30	0	0	30 \pm 0
50	220	0	0	220 \pm 0
100	300	0	0	300 \pm 0
200	438	2.89	0.66	438 \pm 7.19
300	478	2.89	0.60	478 \pm 7.19
400	522	2.89	0.55	522 \pm 7.19
500	640	0	0	640 \pm 0
600	800	0	0	800 \pm 0
700	1000	0	0	1000 \pm 0
800	1020	0	0	1020 \pm 0
900	1078	2.89	0.27	1078 \pm 7.19
1000	1340	0	0	1340 \pm 0
1200	1340	0	0	1340 \pm 0
1500	1500	0	0	1500 \pm 0
1800	1897	5.77	0.30	1897 \pm 14.35
2000	2065	5	0.24	2070 \pm 12.44

Table 12: Range of the used concentration for Hydrochloric acid

Range of used concentration (mMol.L ⁻¹)	Correlation coefficient (r)	r ² %
10-2000	0.9891	97.83
50-2000	0.9911	98.23

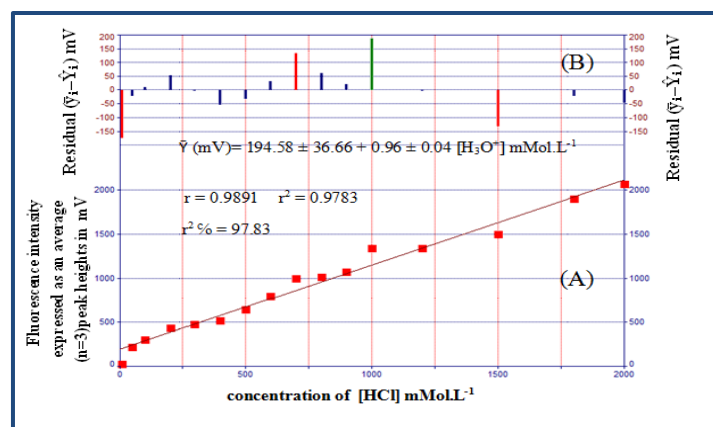


Fig. 15: Scatter plot for the variation of HCl concentration on: A-Fluorescence intensity ,B- residual ($\hat{Y}_i - Y_i$).

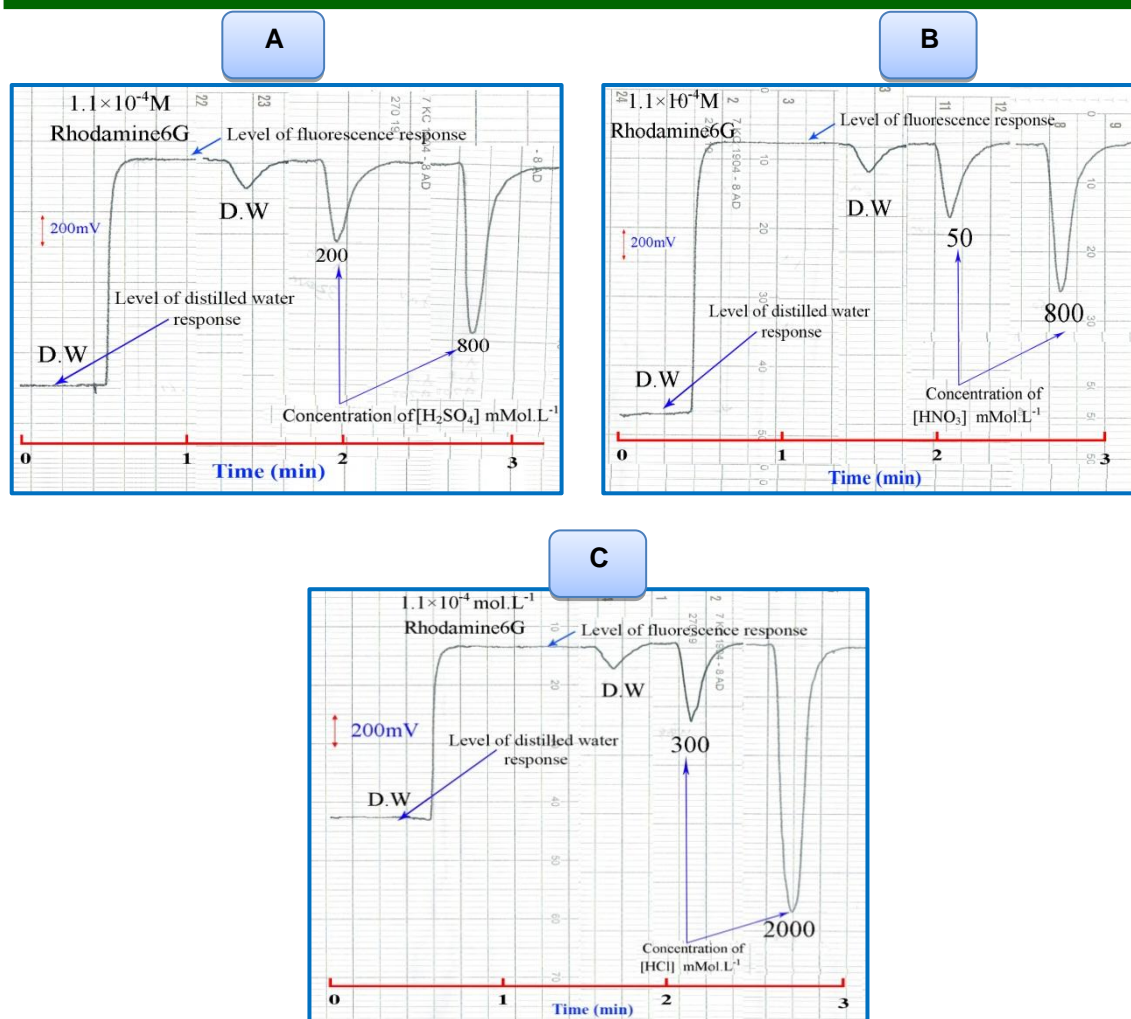


Fig. 16: Effect of variation of $[H_3O^+]$ concentration $mMol.L^{-1}$ (A- H_2SO_4 , B- HNO_3 and C- HCl) on response time profile

4.4.Repeatability of strong acids

The repeatability of measurement and the efficiency of 532nm diode laser and CFI analyzer were studied at fixed concentrations for each one of the used strong acids H_2SO_4 , HNO_3 , and HCl $600 mMol.L^{-1}$ using the optimum parameters (cf. section 3). Repeated measurements for five successive injections were measured; the obtained results are tabulated in Table no. (13) which show that the percentage relative standard deviation was less than 2% which indicates clearly the fluorescence of the adopted methodology using 532 nm diode laser and CFI analyzer gave an acceptable trust ability. Figure no. (17) shows a kind of quenching of fluorescence-time profile for the used concentrations.

Table 13: Repeatability of acids determined via the quenching of fluorescence

Type of acids	No. of times injection to acid $600 mMol.L^{-1}$	Fluorescence intensity quenching expressed as peak height (mV)	Average \bar{y} mV	Standard deviation S.D	Repeatability RSD%	confidence interval of the mean
H_2SO_4	5	780,780, 780, 785,780	781	2.24	0.29	781 ± 2.78
HNO_3	5	1080,1060,1070, 1080,1060	1070	10	0.93	1070 ± 12.39
HCl	5	800,800,800, 820,820	808	10.95	1.36	808 ± 13.57

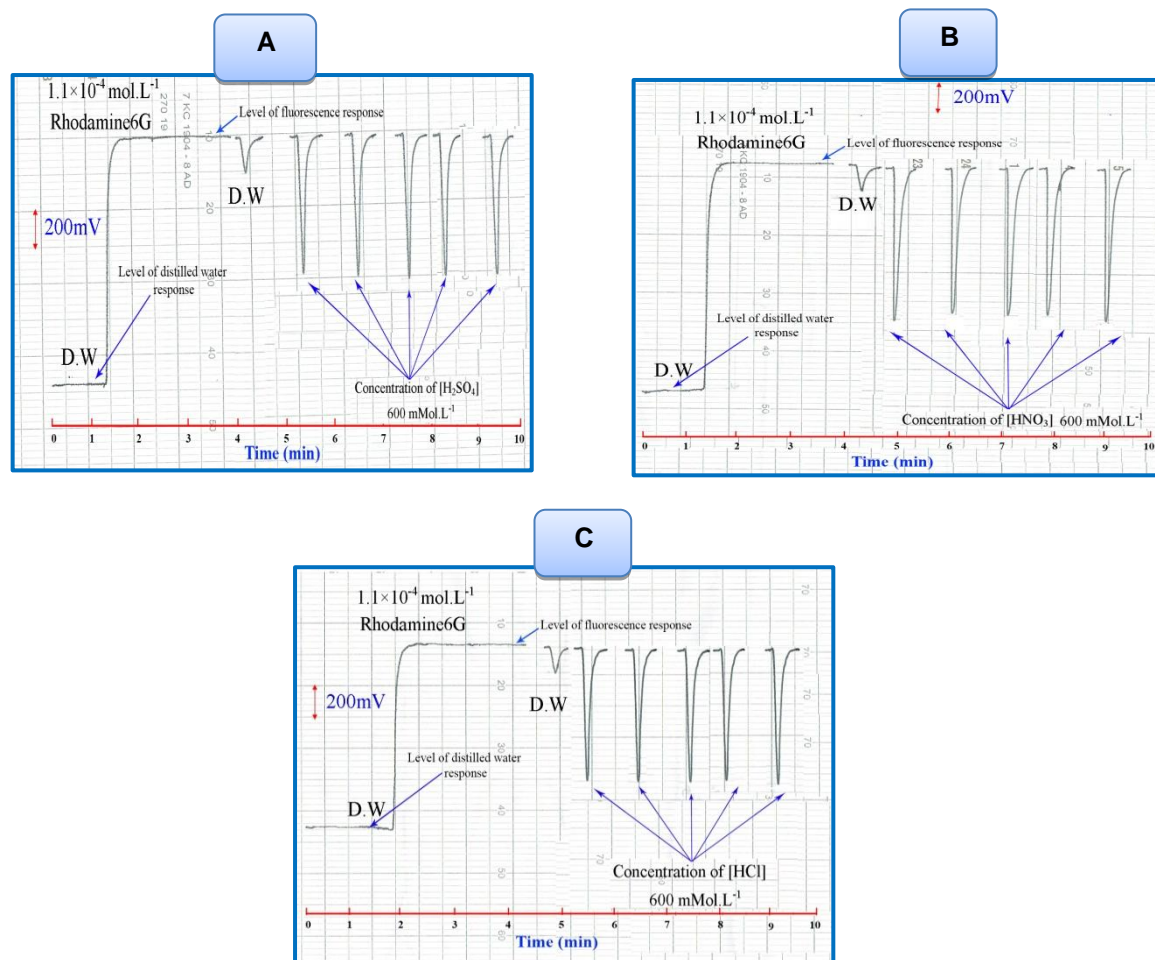


Fig. 17: A Profile of successive repeatability measurements of acids (A: H_2SO_4 , B: HNO_3 , C: HCl (600mMol.L⁻¹) using 532nm solid state laser diode

4.5.Limit of detection for strong acids

Two different methods were used. Gradual dilution of minimum concentration in the calibration graph, or detection based on the numerical value of slope obtained from the linear regression plot. Table no. (14) tabulate all these calculated values of detection limit for 459 μl sample solution. Figure no.(18) Showprofile of detection of limit for Sulfuric acid as a sample of measurements.

Table 14: Limit of detection for acids at optimum condition

Type of acid	K_a for acids	Molecular weight of acids g/mol	minimum concentration (mMol.L ⁻¹)	Practically based on the gradual dilution for the minimum concentration	Theoretical based on the volume of slope $X = 3S_B / \text{slope}$
H_2SO_4	10^3	98.079	6	270.108 $\mu\text{g}/\text{sample}$	1526.913 $\mu\text{g}/\text{sample}$
HNO_3	28	63.01	5	144.608 $\mu\text{g}/\text{sample}$	97.177 $\mu\text{g}/\text{sample}$
HCl	10^6	36.46	9	150.616 $\mu\text{g}/\text{sample}$	117.146 $\mu\text{g}/\text{sample}$

S_B : standard deviation of blank solution. , $X = \text{value of L.O.D based on slope}$. L.O.D = limit of detection

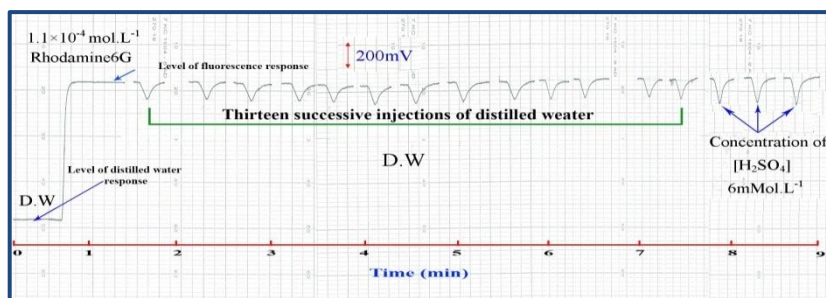


Fig. 18: Profile of detection of limit for Sulfuric acid (6mMol.L⁻¹)

4.6. Application of strong acid

Two different samples of acids (HCl-used in cleaning of cooling devices 1Mol.L^{-1} , H_2SO_4 used in cars batteries 2.5Mol.L^{-1}) were used to analyze and determine $[\text{H}_3\text{O}^+]$. Firstly continuous flow injection analysis using 532nm solid state laser diode while the second method was used the classical measurement for turbidity (Turbidity- HANNA). The standard addition method was applied by preparing a series of solution from HCl by transferring 5ml to five separate volumetric flasks of 25ml, followed by the addition of different aliquots of 0,5,10,15, and 20ml from 1Mol.L^{-1} of HCl and preparing a series of solutions from H_2SO_4 via transferring 2ml to five separate volumetric flasks of 25ml, followed by the addition of 0,2.5,5,7.5, and 10ml from 2Mol.L^{-1} standard solution of H_2SO_4 in order to have the concentration describing the range 0-800mMol.L⁻¹. Using a classical method a series of solution from each acids were prepared by transferring 5ml of HCl 1Mol.L^{-1} to five separate volumetric flasks of 25ml, followed by the addition of 0,5,10,15, and 20ml from 1Mol.L^{-1} standard solution of HCl and transferring 2ml of H_2SO_4 2.5Mol.L^{-1} to five separate volumetric flasks of 25ml, each followed by the addition of 0,2.5,5,7.5, and 10ml from 2Mol.L^{-1} standard solution of H_2SO_4 , then followed by the addition 1ml of lead acetate (0.1mol.L^{-1}) for samples which contain HCl and H_2SO_4 and measured the turbidity for ten volumetric flasks of 25ml for two acids. Table no.(15) shows the summary of standard addition method results from two samples using two methods newly method and classical method (Turbidity- HANNA). A straight-line graph from 0-800mMol.L⁻¹ was obtained (figure no.19). Table no.(16) summarizes paired t-test between newly method and classical method (Turbidity- HANNA); in commercial samples. The obtained results indicate that there were no significant differences between the proposed method and the classical method at 95% confidence interval as the calculated t-value is less than tabulated critical t-value for hydrochloric and sulfuric acids. On this basis the new method using can be used as an alternative method for the determination of $[\text{H}_3\text{O}^+]$ ion in commercial formulations.

Table 15: Standard additions method for the determination of $[\text{H}_3\text{O}^+]$ by 532nm solid state laser diode and (Turbidity- HANNA) method

532nm solid state laser diode					
(Turbidity- HANNA)					
Concentration of acids [HCl] and $[\text{H}_2\text{SO}_4]$ mMol.L ⁻¹ (0,200,400,600,800)					
Standard value of acids HCl 1000 mMol.L ⁻¹ and H_2SO_4 2500mMol.L ⁻¹					
Type of acid	$\hat{y} = a \pm S_a t + b \pm S_b t$ [X] at confidence interval at 95%, n-2	r r ² %	t _{tab} at 95% Confidence interval, n-2	Calculate t-value = $\frac{r/\sqrt{n-2}}{\sqrt{1-r^2}}$	Practical concentration mMol.L ⁻¹ in 25ml In prepared sample 25ml (1Mol.L ⁻¹) HCl and (2.5Mol.L ⁻¹) H_2SO_4
HCl	$220 \pm 84.05 + 1.13 \pm 0.17$ [HCl] mMol.L ⁻¹	0.9671 0.9353 93.53%	3.182	6.59 3.182 << 6.59	194.69 973.45
H_2SO_4	$293 \pm 77.99 + 1.45 \pm 0.16$ [H_2SO_4] mMol.L ⁻¹	0.9823 0.9649 96.49%		9.77 3.182 << 6.59	202.07 2525.88
HCl	$201 \pm 76.01 + 1.07 \pm 0.16$ [HCl] mMol.L ⁻¹	0.9696 0.9401 94.01%	3.182	6.86 3.182 << 6.86	187.85 939.25
H_2SO_4	$210.60 \pm 62.81 + 1.05 \pm 0.13$ [H_2SO_4] mMol.L ⁻¹	0.9784 0.9573 95.73%		8.21 3.182 << 8.21	200.57 2507.13

[X] Concentration of $[\text{H}_3\text{O}^+]$ (mMol.L⁻¹) r: Correlation coefficient, r²: Coefficient of determination and r² %: linearity percentage, \hat{y} : Estimated response value (mV for 532nm solid state laser diode and Turbidity- HANNA method).

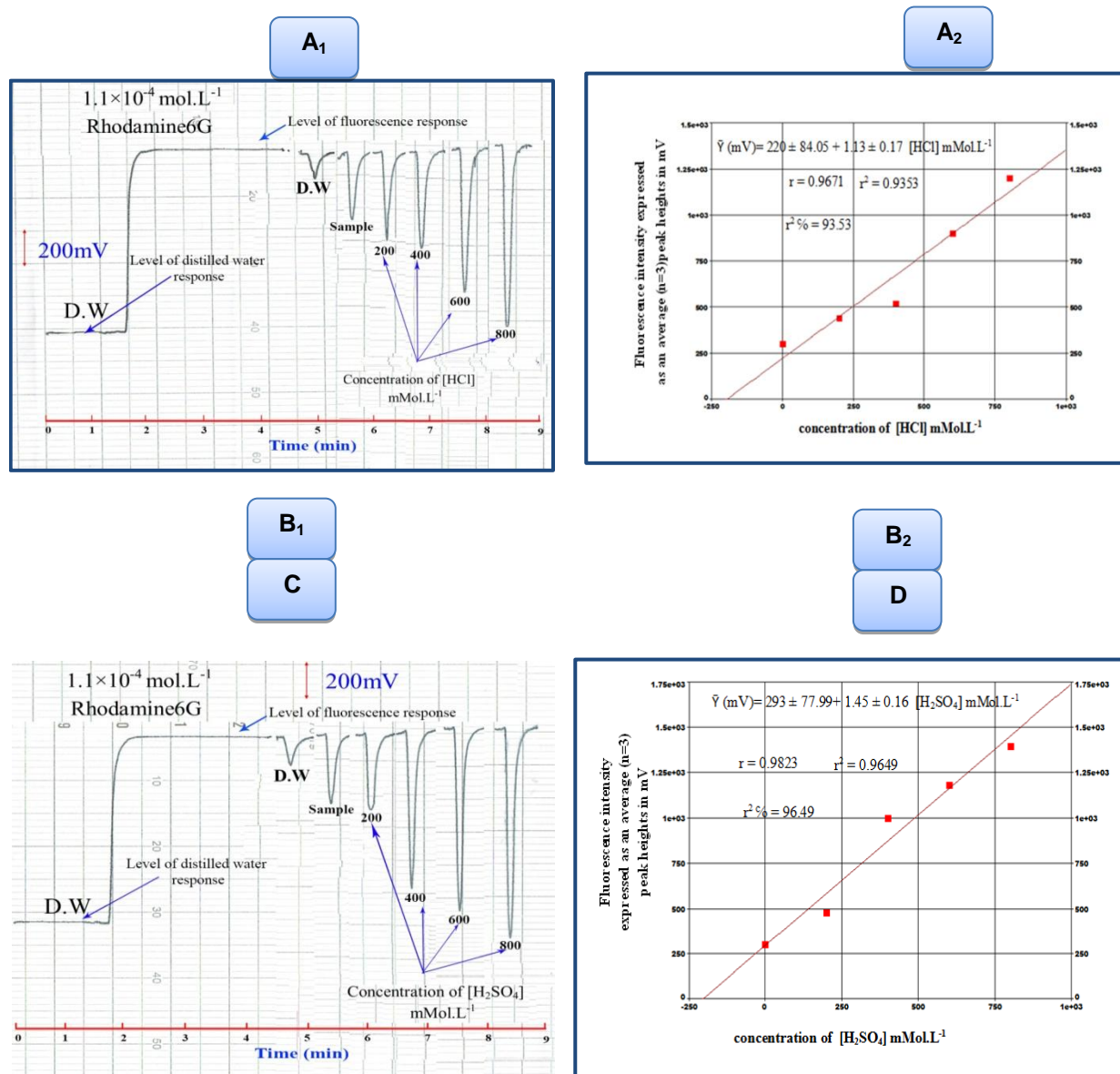


Fig. 19: Standard addition calibration graph and sample of response profile and standard addition calibration plot for two acids A₁, A₂ HCl used in cleaning of cooling devices and B₁, B₂ H₂SO₄ used in cars batteries using 532 nm solid state laser diode method and C HCl used in cleaning of cooling devices, D H₂SO₄ used in cars batteries using (Turbidity- HANNA) method

Table 16: Paired t-test for comparison between standard value and two acids

Standard value(mMol.L ⁻¹)	532nm solid state laser diode (Turbidity- HANNA)			
	(HCl)		H ₂ SO ₄	
1-1000mMol.L ⁻¹ (HCl)	973.45		2525.88	
	939.25		2507.13	
2-2500mMol.L ⁻¹ (H ₂ SO ₄)	X _{1d} = 43.65		X _{1d} = 16.505	
	σ _{n-1} = 25.14		σ _{n-1} = 13.26	
	N = 2		N = 2	
	Df = 1		Df = 1	
	$t_{cal} = X_d \sqrt{n} / \sigma_{n-1}$		$t_{cal} = X_d \sqrt{n} / \sigma_{n-1}$	
	t _{lab} at 95% = t _{0.05/2} for n = 2		t _{lab} at 95% = t _{0.05/2} for n = 2	
	2.448 << 12.706		1.755 << 12.706	

X_{1d}: average difference between HCl with standard value, X_{2d}: average difference between H₂SO₄ with standard value, N: no of measurements, df: degree of freedom, σ_{n-1}: Standard deviation for concentration.

CONCLUSIONS

Through the work that has been conducted, it can be clearly noticed that a clear trust of liable determination can be processed through the methodology adopted in this research work. The RSD% less than 2% was observed for all samples, indicating a satisfactory precision of the proposed method. Therefore the adopted method can be regarded as an alternative simple method for the determination of Hydronium ion in strong acids.

REFERENCES

1. Hosoda K, Furuta T and Ishii K. Simultaneous determination of glucuronic acid and sulfuric acid conjugated metabolites of daidzein and genistein in human plasma by high-performance liquid chromatography. *Journal of Chromatograph*. 2010;878(78):628-636.
2. Wenke W, Jörg A and Iris G. Determination of total fluoride in HF/HNO₃/H₂SiF₆ each solutions by new potentiometric titration methods. *Talanta*. 2007;71(5):1901-5.
3. Bucker S and Acker J. Spectrometric analysis of process eating solutions of the photovoltaic industry-determination of HNO₃, HF and H₂SiF₆ using high-resolution continuum source absorption spectrometry of diatomic molecules and atoms. *Talanta*. 2012;94:335-341.
4. Noriyoshi M, Toshihiko U, Masahiro K and Shigeko Y. Gas Chromatographic Determination of Sulfuric Acid and Application to Urinary Sulfate. *Acta Medica Okayama*. 1988;42(5).
5. Issam MSA and Hussien. New mode for the on-line determination of Oxonium ion in different strong acids using CFIA via the use of homemade linear array Ayah 5Sx4-ST- 5D solar CFI analyser, Iraq journal for science. 2015;56 (1B).
6. Issam MSA and Hussien. Novel semi-automated on-line determination of Oxonium ion via precipitation reaction using a new mode of attenuated measurement of incident light (0-180°) by AYAH 5SX4-ST- 5D solar CFI analyser, Iraq journal for science. 2014;55(4B).
7. Issam MA Shakir and Ra'ed Falih Hassan. A Novel Method for the Determination of Oxonium Ion in Strong Acids Via Flow Injection Chemiluminescence. *Iraq journal for science*. 2008.
8. Shakir IMA and Mansoor AA. Novel method for determination of Hydrochloric acid via ion exchange and precipitation reaction indirectly by using linear array Ayah 5SX1-T-1D continuous flow injection analyser. *International Journal of Pharmacy and Chemistry*. 2014; 4(4):763-776.
9. Shakir IMA and Mansoor AA. New Approach for The Turbidimetric Determination of Hydronium ion by Using Homemade Linear Array Ayah 5SX1-T-1D-CFI Analyser", *Iraq journal for science*. 2014;4B (55).
10. Schäfer FP.(Ed.), *Dye Lasers*, 3rd Ed. (Springer-Verlag, Berlin, 1990).
11. Duarte FJ and Hillman (Eds.) LW. *Dye Laser Principles* (Academic, New York, 1990).
12. Birge RR. *Kodak Laser Dyes*. Kodak publication. 1987;169.
13. Starchura S and Allison J. Identification of organic pigments in automotive coatings using laser desorption mass spectrometry. *J Forens Sci*. 2007;52(3):595-603.
14. Snavely BB and Continuous-Wave Dye Laser I. in *Topics in Appl Phys*. 1989;1.
15. Drexhage KH. Structure and properties of laser dyes, *Laser Focus*. 1973;3:35-36.
16. Drexhage K and *Dye Lasers*. Edited by F P Schafer, Springer-Verlag, Berlin. 1990;167-173.
17. Brackmann U. *Lambda chrome Laser Dyes*, *Lambda Physik*, Germany. 1994;27-213.
18. Huber G, Kränkel C and Petermann K. Solid-state lasers: status and future. *JOSA B*. 2010; 27(11): B93.
19. Byer RL. Diode laser-pumped solid-state lasers. *Science*. 1988;239:742.
20. Walter Koechne; Michael Bass. *Solid-State Lasers: A Graduate Text*. Springer: New York, 44-77.
21. Koechner W. *Solid-State Laser Engineering*, 6th edn., Springer, Berlin. 2006.